

UAV-enabled Secure Communication with Finite Blocklength

Yuntian Wang¹, Xiaobo Zhou¹, Zhihong Zhuang^{1*}, Linlin Sun¹, Yuwen Qian¹,
Jinhui Lu¹ & Feng Shu^{1*}

¹*School of Electronic and Optical Engineering, Nanjing University of Science and Technology, Nanjing 210094, China*

Abstract In the finite blocklength scenario, which is suitable for practical applications, a method of maximizing the average effective secrecy rate (AESR), significantly distinct from the infinite case, is proposed to optimize the UAV trajectory and transmit power subject to UAV mobility constraints and transmit power constraints. To address the formulated non-convex optimization problem, it is first decomposed into two non-convex subproblems. Then the two subproblems are converted respectively into two convex subproblems via the first-order approximation. Finally, an alternating iteration algorithm is developed by solving the two subproblems iteratively using successive convex approximation (SCA) technique. Numerical results show that our proposed scheme achieves a better AESR performance than a benchmark scheme.

Keywords UAV communications, Physical Layer Security, Trajectory Optimization, Transmit Power Optimization, Finite Blocklength.

Citation .
. Sci China Inf Sci, for review

1 Introduction

In recent years, with the rapid development of unmanned aerial vehicles (UAVs) manufacturing, the functions of UAVs have become diversified, and they are playing an increasingly important role in the fields of military, search, rescue, surveillance, cargo delivery, telecommunications, etc. Especially in the field of telecommunications, UAVs have been considered as one of the significant component of the fifth generation (5G) wireless system due to the advantages of low cost, high mobility, flexible deployment and high probabilities of line of sight (LoS) channels [1–4], which attracts extensive attention from industry and academia. For example, in industry, Qualcomm have joined forces with AT&T to trial UAVs operation on AT&T's commercial networks to accelerate wide-scale wireless coverage [5], and they have worked together to optimize the commercial networks for UAV communications to pave the path to 5G [6]. At the same time, in academia, a lot of effort has been made in the research of UAV networks, and many valuable research results have been achieved. For example, in [7], a UAV was deployed to serve as a aerial base station to communicate with ground users in time division multiple access (TDMA) manner. By optimizing the UAV trajectory and user scheduling, the max-min average rate can be achieved. Furthermore, the scenario of multi-UAV operating in a cooperation manner was considered in [8]. In addition to acting as the aerial base station, UAV can also act as the mobile relay when there is no direct link between transmitter and receiver [9]. Besides, in recent work [10], a UAV is deployed as the mobile data collector to collect data from sensor nodes. Moreover, taking energy efficiency into

* Corresponding author (email: nustcn@163.com, shufeng@njjust.edu.cn)

consideration [11], the authors of [12] aimed to maximize the energy efficiency of UAV networks by optimizing UAV's trajectory.

On the other hand, note that the traditional terrestrial wireless communications are vulnerable to malicious wiretap and attack due to the nature of broadcast. Thus, a lot of methods have been proposed to safeguard the physical layer security (PLS) of communications [13–20], such as massive multiple-input multiple-output (MIMO), directional modulation, precise transmission, and artificial noise. Meanwhile, the potential eavesdropping and attack on UAV networks are more serious due to the air-to-ground LoS channel. Consequently, the communication security of UAV networks has also been widely investigated. For instance, the authors of [21] tried to maximize the secrecy rate through jointly optimizing the UAV's trajectory and transmit power. To further improve PLS performance, the authors of [22] considered the case of two UAVs, in which one was used to transmit confidential information (CI) while the other was used to transmit the artificial noise (AN) to prevent eavesdroppers (Eves) from wiretapping. Furthermore, unlike traditional PLS technologies that devote to improving the secrecy rate, covert communications are dedicated to hiding the transmission behavior of the transmitter, which can provide high-level security [23, 24]. As a result, [25] combined the UAV networks with covert communications, where the UAV's trajectory and transmit power were optimized to maximize the average covert transmission rate under the transmission outage and covertness constraints.

However, the aforementioned literatures related to PLS all assumed that CI has infinite blocklength. This assumption is impractical and can not meet the demands of some applications for 5G wireless system on ultra-reliable and low-latency communication (URLLC), such as factory automation and autonomous vehicles, which require at least 99.999% reliability within 1 ms end-to-end latency [26–28]. As a result, the packet with finite blocklength will be used to meet the both stringent requirements on reliability and latency. Under this condition, the law of large numbers is no longer true, and the thermal noise and the distortions at the receiver can not be averaged out [29]. Consequently, the expression of secrecy rate which leading to the results of [21, 22, 25] can not be used directly [30].

Motivated by the above reasons, in this paper, we study the UAV-enabled secure communication with finite blocklength, where a UAV is used to transmit CI with finite blocklength to the legitimate user (Bob) in the existence of Eve. The main contributions of this paper are summarized as follows.

- For the first time, we consider the secure UAV communication with finite blocklength. The results of information theory on finite blocklength bounds for wiretap channels are utilized to approximate the average effective secrecy rate (AESR) of the considered system, which are quite different from the results of the aforementioned works considering the infinite blocklength.
- We aim to maximize AESR subject to the UAV's mobility and transmit power constraints by jointly optimizing the UAV's trajectory and transmit power. However, the formulated optimization problem is non-convex and thus difficult to solve directly. Therefore, we first decompose the optimization problem into two non-convex subproblems. Then the two subproblems are transformed into convex ones based on the first-order approximation. Finally, an alternating iteration algorithm based on successive convex approximate (SCA) technique is proposed to solve the formulated problem.
- Numerical results show that the proposed alternating iterative algorithm can significantly outperform the benchmark scheme from the perspective of AESR. Besides, we can observe that the UAV trajectory obtained by the proposed scheme tends to fly away from Eve to degrade Eve's wiretap and thus improve the communication security.

The remainder of this paper is organized as follows: In Section 2, we present the system model and formulate the optimization problem. An alternating iterative algorithm is proposed in Section 3 to solve the formulated optimization problem. Numerical results are provided in Section 4 to demonstrate the effectiveness of our proposed algorithm. Finally, the conclusions are drawn in Section 5.

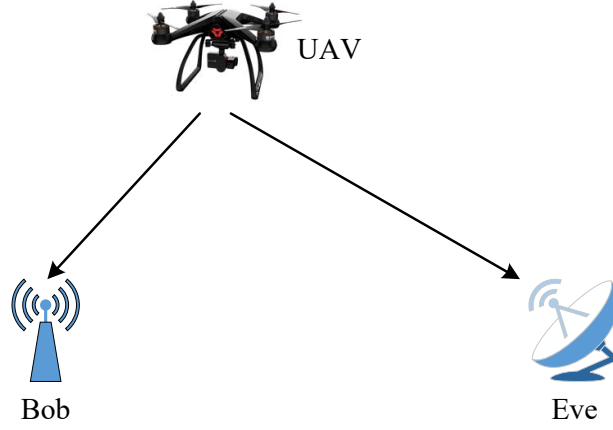


Figure 1 UAV-enabled secure communication system with finite blocklength.

2 System Model and Problem Formulation

2.1 System Model

As shown in Fig. 1, we consider a UAV-enabled secure wireless communication system, where a UAV is served as an aerial base station to transmit CI to Bob, while a potential Eve tries to wiretap CI. In contrast to the conventional UAV-enabled secure wireless communication systems where infinite blocklength is assumed for CI, we consider the case of CI with finite blocklength. For ease of presentation, we consider a three dimension (3D) Cartesian coordinate system, where Bob and Eve are located at $\mathbf{w}_b = [x_b, y_b, 0]^T$ and $\mathbf{w}_e = [x_e, y_e, 0]^T$, respectively. The trajectory of UAV within flight duration T can be expressed as $\mathbf{q}(t) = [x(t), y(t), H]^T$, $0 \leq t \leq T$, where H denotes the fixed flight altitude. For the sake of simplicity, the flight duration T is equally divided into N time slots with duration $\delta_t = \frac{T}{N}$. As a result, the trajectory of UAV can be discretized as a sequence $\mathbf{q}[n] = [x[n], y[n], H]^T$, $1 \leq n \leq N$. Then, the mobility constraints of UAV are given by

$$\|\mathbf{q}[n+1] - \mathbf{q}[n]\| \leq V_{\max} \delta_t, n = 1, 2, \dots, N-1, \quad (1a)$$

$$\mathbf{q}[1] = \mathbf{q}_I, \quad \mathbf{q}[N] = \mathbf{q}_F, \quad (1b)$$

where V_{\max} denotes the maximum flight speed of UAV, $\mathbf{q}_I = [x_I, y_I, H]^T$ and $\mathbf{q}_F = [x_F, y_F, H]^T$ denote the predetermined initial and final location of UAV, respectively. It is worth mentioning that the duration of each time slot δ_t should be carefully considered. Firstly, δ_t should be sufficient small so that the UAV can be treated as static within each time slot. Secondly, δ_t is greater than the time it takes to send one block.

In this paper, all the nodes are assumed to be equipped with single antenna. Besides, we assume that the communication links from UAV to Bob and Eve are dominated by LoS. Furthermore, the Doppler effect caused by the motion of UAV is assumed to be perfectly compensated at Bob and Eve. Consequently, the channel power gain from UAV to Bob in time slot n can be expressed as

$$h_b[n] = \zeta_0 d_b^{-2}[n] = \frac{\zeta_0}{\|\mathbf{q}[n] - \mathbf{w}_b\|^2}, \forall n, \quad (2)$$

where $d_b[n] = \|\mathbf{q}[n] - \mathbf{w}_b\|$ denotes the distance from UAV to Bob in time slot n , and ζ_0 denotes the channel power gain at the reference distance $d_0 = 1$ m. Similarly, the channel power gain from UAV to Eve in time slot n can be expressed as

$$h_e[n] = \zeta_0 d_e^{-2}[n] = \frac{\zeta_0}{\|\mathbf{q}[n] - \mathbf{w}_e\|^2}, \forall n, \quad (3)$$

where $d_e[n] = \|\mathbf{q}[n] - \mathbf{w}_e\|$ denotes the distance from UAV to Eve in time slot n . Assume that the transmit power of UAV in time slot n is denoted as $P[n]$. Taking the average and instantaneous power limits into

accountant [21], the transmit power constraints are given by

$$\frac{1}{N} \sum_{n=1}^N P[n] \leq \bar{P}, \quad (4a)$$

$$0 \leq P[n] \leq P_{\max}, \forall n, \quad (4b)$$

where \bar{P} and P_{\max} denote the maximum average and instantaneous transmit power, respectively. Then, according to [30] and [31], a lower bound on the secrecy rate in bits per channel use (BPCU) in time slot n can be approximated as

$$R_s[n] = \left[\log_2(1 + \gamma_b[n]) - \log_2(1 + \gamma_e[n]) - \sqrt{\frac{V_b[n]}{L}} \frac{Q^{-1}(\varepsilon)}{\ln 2} - \sqrt{\frac{V_e[n]}{L}} \frac{Q^{-1}(\epsilon)}{\ln 2} \right]^+, \forall n, \quad (5)$$

where the operation $[x]^+ \triangleq \max\{x, 0\}$, and $Q^{-1}(x)$ is the inverse of the Gaussian Q-function $Q(x) \triangleq \int_x^\infty \frac{1}{\sqrt{2\pi}} e^{-\frac{t^2}{2}} dt$. We note that L in (5) denotes the blocklength, ε and ϵ denote the decoding error probability at Bob and the information leakage at Eve, respectively. $\gamma_b[n]$ and $\gamma_e[n]$ in (5) given by

$$\gamma_b[n] = \frac{P[n]h_b[n]}{\sigma^2} = \frac{\xi_0 P[n]}{\|\mathbf{q}[n] - \mathbf{w}_b\|^2}, \forall n, \quad (6)$$

$$\gamma_e[n] = \frac{P[n]h_e[n]}{\sigma^2} = \frac{\xi_0 P[n]}{\|\mathbf{q}[n] - \mathbf{w}_e\|^2}, \forall n, \quad (7)$$

denote the signal-to-noise ratios (SNRs) at Bob and Eve, respectively, where σ^2 is the additive white Gaussian noise (AWGN) power at Bob and Eve, and $\xi_0 = \frac{\zeta_0}{\sigma^2}$. $V_b[n]$ is the channel dispersion of Bob in time slot n , which is given by [30, 31]

$$V_b[n] = 1 - (1 + \gamma_b[n])^{-2}, \forall n. \quad (8)$$

Similarly, $V_e[n]$ denotes the channel dispersion of Eve in time slot n , which is given by

$$V_e[n] = 1 - (1 + \gamma_e[n])^{-2}, \forall n. \quad (9)$$

As per (5), the average secrecy rate over N time slots is given by

$$R_s = \frac{1}{N} \sum_{n=1}^N R_s[n]. \quad (10)$$

2.2 Problem Formulation

Note that the decoding error probability at Bob can not be neglected due to the finite blocklength. As such, our target is to maximize AESR [31] given by $R_s(1 - \varepsilon)$ via jointly optimizing the trajectory and the transmit power of UAV under the mobility constraints and the transmit power constraints. The resultant optimization problem is formulated as

$$\max_{\mathbf{Q}, \mathbf{P}} R_s(1 - \varepsilon) \quad (11a)$$

$$\text{s.t. (1), (4),} \quad (11b)$$

where $\mathbf{Q} = \{\mathbf{q}[n], \forall n\}$ is the UAV trajectory and $\mathbf{P} = \{P[n], \forall n\}$ is the transmit power of UAV over N time slots. In (11a), the operation $[x]^+$ is removed because if there exist some time slot n making $R_s[n] < 0$, we can always set $P[n] = 0$ and then increase $R_s[n]$ to 0 without violating the power constraints (4). We note that problem (11) is non-convex and difficult to solve optimally due to the fact that the expression of R_s is very complicated as well as \mathbf{Q} and \mathbf{P} are closely coupled in the objective function. As such, in the next section, we propose an efficient algorithm to find a suboptimal solution to problem (11).

3 Alternating Iterative Algorithm for Problem (11)

To facilitate processing problem (11), we introduce slack variables $\mathbf{U}_b = \{u_b[n], \forall n\}$, $\mathbf{U}_e = \{u_e[n], \forall n\}$, $\mathbf{Z}_b = \{z_b[n], \forall n\}$ and $\mathbf{Z}_e = \{z_e[n], \forall n\}$, then problem (11) can be reformulated as

$$\max_{\substack{\mathbf{Q}, \mathbf{P}, \mathbf{U}_b, \\ \mathbf{U}_e, \mathbf{Z}_b, \mathbf{Z}_e}} \frac{1}{N} \sum_{n=1}^N \tilde{R}_s[n](1 - \varepsilon) \quad (12a)$$

$$\text{s.t. (1), (4),} \quad (12b)$$

$$u_b[n] \geq \frac{\xi_0 P[n]}{\|\mathbf{q}[n] - \mathbf{w}_b\|^2}, \forall n, \quad (12c)$$

$$u_e[n] \geq \frac{\xi_0 P[n]}{\|\mathbf{q}[n] - \mathbf{w}_e\|^2}, \forall n, \quad (12d)$$

$$z_b^2[n] \geq 1 - (1 + u_b[n])^{-2}, \forall n, \quad (12e)$$

$$z_e^2[n] \geq 1 - (1 + u_e[n])^{-2}, \forall n, \quad (12f)$$

$$z_b[n] \geq 0, \forall n, \quad (12g)$$

$$z_e[n] \geq 0, \forall n. \quad (12h)$$

where

$$\tilde{R}_s[n] = \log_2 \left(1 + \frac{\xi_0 P[n]}{\|\mathbf{q}[n] - \mathbf{w}_b\|^2} \right) - \log_2(1 + u_e[n]) - z_b[n] \frac{Q^{-1}(\varepsilon)}{\sqrt{L} \ln 2} - z_e[n] \frac{Q^{-1}(\epsilon)}{\sqrt{L} \ln 2}, \forall n. \quad (13)$$

We note that problem (12) is equivalent to problem (11) since the constraints (12c)-(12f) hold with equality at the optimal solution. However, problem (12) is still non-convex and hard to solve because the objective function (12a) is non-concave with respect to (w.r.t.) \mathbf{Q} , \mathbf{P} and \mathbf{U}_e . Besides, constraints (12c)-(12f) are non-convex. As a result, in the following, we first decompose problem (12) into two subproblems, then we transform the two subproblems into convex optimization problems, and finally we develop an alternating iteration algorithm and employ the SCA technique to solve the formulated problem.

3.1 Trajectory Optimization

For given feasible transmit power \mathbf{P} , problem (12) can be simplified as

$$\max_{\substack{\mathbf{Q}, \mathbf{U}_b, \\ \mathbf{U}_e, \mathbf{Z}_b, \mathbf{Z}_e}} \frac{1}{N} \sum_{n=1}^N \tilde{R}_s[n](1 - \varepsilon) \quad (14a)$$

$$\text{s.t. (1), (12c) - (12h).} \quad (14b)$$

However, problem (14) is still non-convex because the objective function (14a) is non-concave, and constraints (12c)-(12f) are non-convex. In the following, we focus on transforming problem (14) into a convex optimization problem.

To this end, we introduce slack variable $\mathbf{L}_b = \{l_b[n], \forall n\}$ and equivalently rewrite constraint (12c) as

$$u_b[n] \geq \frac{\xi_0 P[n]}{l_b[n]}, \forall n, \quad (15a)$$

$$\|\mathbf{q}[n] - \mathbf{w}_b\|^2 \geq l_b[n], \forall n. \quad (15b)$$

Note that constraint (15a) is convex now, but constraint (15b) is still non-convex due to the superlevel of a convex function. It is well known that a convex (concave) function is lower (upper) bounded by its first-order Taylor expansion. This motivates us to use the first-order approximation technique to tackle

the non-convex constraint (15b). Specifically, the term $\|\mathbf{q}[n] - \mathbf{w}_b\|^2$ can be replaced by its first-order Taylor expansion. Thus, for given feasible point $\hat{\mathbf{q}}[n]$, constraint (15b) can be approximated as

$$\|\hat{\mathbf{q}}[n] - \mathbf{w}_b\|^2 + 2(\hat{\mathbf{q}}[n] - \mathbf{w}_b)^T(\mathbf{q}[n] - \hat{\mathbf{q}}[n]) \geq l_b[n], \forall n, \quad (16)$$

which is a convex constraint. So far, the non-convex constraint (12c) has been approximated as the convex constraints (15a) and (16). Similarly, by introducing slack variable $\mathbf{L}_e = \{l_e[n], \forall n\}$, the non-convex constraint (12d) can be approximated as convex constraints

$$u_e[n] \geq \frac{\xi_0 P[n]}{l_e[n]}, \forall n, \quad (17)$$

and

$$\|\hat{\mathbf{q}}[n] - \mathbf{w}_e\|^2 + 2(\hat{\mathbf{q}}[n] - \mathbf{w}_e)^T(\mathbf{q}[n] - \hat{\mathbf{q}}[n]) \geq l_e[n], \forall n. \quad (18)$$

For constraint (12e), we observe that it is in the form of a superlevel of a convex function, which can be approximated by its first-order convex approximation. Consequently, for given feasible points $\hat{z}_b[n]$ and $\hat{u}_b[n]$, constraint (12e) can be approximated as

$$\hat{z}_b^2[n] + 2\hat{z}_b[n](z_b[n] - \hat{z}_b[n]) \geq 1 - (1 + \hat{u}_b[n])^{-2} + 2(1 + \hat{u}_b[n])^{-3}(u_b[n] - \hat{u}_b[n]), \forall n. \quad (19)$$

Similarly, constraint (12f) can be approximated as constraint

$$\hat{z}_e^2[n] + 2\hat{z}_e[n](z_e[n] - \hat{z}_e[n]) \geq 1 - (1 + \hat{u}_e[n])^{-2} + 2(1 + \hat{u}_e[n])^{-3}(u_e[n] - \hat{u}_e[n]), \forall n, \quad (20)$$

where $\hat{z}_e[n]$ and $\hat{u}_e[n]$ are given feasible points.

For the objective function (14a), we observe that $\tilde{R}_s[n]$ in the objective function is jointly convex w.r.t. $\|\mathbf{q}[n] - \mathbf{w}_b\|^2$ and $u_b[n]$. Consequently, the first-order approximation technique can be used to construct a lower bound of $\tilde{R}_s[n]$, which can be expressed as

$$\begin{aligned} \tilde{R}_s[n] \geq & \log_2 \left(1 + \frac{\xi_0 P[n]}{\|\hat{\mathbf{q}}[n] - \mathbf{w}_b\|^2} \right) - \frac{\xi_0 P[n](\|\mathbf{q}[n] - \mathbf{w}_b\|^2 - \|\hat{\mathbf{q}}[n] - \mathbf{w}_b\|^2)}{(\|\hat{\mathbf{q}}[n] - \mathbf{w}_b\|^2)(\|\hat{\mathbf{q}}[n] - \mathbf{w}_b\|^2 + \xi_0 P[n]) \ln 2} - \\ & \log_2(1 + \hat{u}_e[n]) - \frac{u_e[n] - \hat{u}_e[n]}{(1 + \hat{u}_e[n]) \ln 2} - z_b[n] \frac{Q^{-1}(\varepsilon)}{\sqrt{L} \ln 2} - z_e[n] \frac{Q^{-1}(\epsilon)}{\sqrt{L} \ln 2} \triangleq \tilde{R}_{s,q}^{lb}[n], \forall n. \end{aligned} \quad (21)$$

Following the above transformation, problem (14) can be reformulated as

$$\max_{\substack{\mathbf{Q}, \mathbf{U}_b, \mathbf{U}_e, \\ \mathbf{Z}_b, \mathbf{Z}_e, \mathbf{L}_b, \mathbf{L}_e}} \frac{1}{N} \sum_{n=1}^N \tilde{R}_{s,q}^{lb}[n](1 - \varepsilon) \quad (22a)$$

$$\text{s.t. (1), (12g), (12h), (15a), (16) - (20).} \quad (22b)$$

Problem (22) is now a convex optimization problem, which can be efficiently solved by optimization tools such as CVX [32].

3.2 Transmit Power Optimization

For given feasible UAV trajectory \mathbf{Q} , problem (12) can be simplified as

$$\max_{\mathbf{P}, \mathbf{U}_b, \mathbf{U}_e, \mathbf{Z}_b, \mathbf{Z}_e} \frac{1}{N} \sum_{n=1}^N \tilde{R}_s[n](1 - \varepsilon) \quad (23a)$$

$$\text{s.t. (4), (12c) - (12h).} \quad (23b)$$

Obviously, problem (23) is non-convex due to the convexity of the second term of $\tilde{R}_s[n]$ and the non-convexity of constraints (12e) and (12f). Similar to the process in the previous subsection, constraints (12e) and (12f) can be approximated as constraint (19) and (20), respectively. For the objective function

Algorithm 1 Alternating iterative algorithm for problem (11)

-
- 1: Initialize $\{\mathbf{Q}^0, \mathbf{P}^0, \mathbf{U}_b^0, \mathbf{U}_e^0, \mathbf{Z}_b^0, \mathbf{Z}_e^0\}$; Let $r = 0$.
 - 2: **repeat**
 - 3: Solve problem (22) for given $\{\mathbf{Q}^r, \mathbf{P}^r, \mathbf{U}_b^r, \mathbf{U}_e^r, \mathbf{Z}_b^r, \mathbf{Z}_e^r\}$ and obtain the optimal solution $\{\mathbf{Q}^{r+1}, \mathbf{U}_b^{r+1}, \mathbf{U}_e^{r+1}, \mathbf{Z}_b^{r+1}, \mathbf{Z}_e^{r+1}\}$.
 - 4: Let $\{\mathbf{U}_b^r, \mathbf{U}_e^r, \mathbf{Z}_b^r, \mathbf{Z}_e^r\} = \{\mathbf{U}_b^{r+1}, \mathbf{U}_e^{r+1}, \mathbf{Z}_b^{r+1}, \mathbf{Z}_e^{r+1}\}$.
 - 5: Solve problem (25) for given $\{\mathbf{Q}^{r+1}, \mathbf{U}_b^r, \mathbf{U}_e^r, \mathbf{Z}_b^r, \mathbf{Z}_e^r\}$ and obtain the optimal solution $\{\mathbf{P}^{r+1}, \mathbf{U}_b^{r+1}, \mathbf{U}_e^{r+1}, \mathbf{Z}_b^{r+1}, \mathbf{Z}_e^{r+1}\}$.
 - 6: Let $r = r + 1$.
 - 7: **until** the fractional increase of the objective function is below a threshold τ .
-

(23a), we can employ the first-order approximation to construct a lower bound of $\tilde{R}_s[n]$, which is detailed as

$$\begin{aligned} \tilde{R}_s[n] \geq & \log_2 \left(1 + \frac{\xi_0 P[n]}{\|\mathbf{q}[n] - \mathbf{w}_b\|^2} \right) - \log_2(1 + \hat{u}_e[n]) - \\ & \frac{u_e[n] - \hat{u}_e[n]}{(1 + \hat{u}_e[n]) \ln 2} - z_b[n] \frac{Q^{-1}(\varepsilon)}{\sqrt{L} \ln 2} - z_e[n] \frac{Q^{-1}(\epsilon)}{\sqrt{L} \ln 2} \triangleq \tilde{R}_{s,p}^{lb}[n], \forall n. \end{aligned} \quad (24)$$

Then, problem (23) can be approximated as

$$\max_{\mathbf{P}, \mathbf{U}_b, \mathbf{U}_e, \mathbf{Z}_b, \mathbf{Z}_e} \frac{1}{N} \sum_{n=1}^N \tilde{R}_{s,p}^{lb}[n] (1 - \varepsilon) \quad (25a)$$

$$\text{s.t. (4), (12c), (12d), (12g), (12h), (19), (20).} \quad (25b)$$

We note that problem (25) is a convex optimization problem, which can be efficiently solved by CVX [32].

3.3 Overall Algorithm

In the previous two subsections, we have transformed the trajectory optimization subproblem and the transmit power optimization subproblem into convex optimization problems. In this subsection, we develop an alternating iteration algorithm based on the SCA technique to solve the two subproblems alternatively. Following the principle of the SCA technique, at each iteration, the current optimal solution to each subproblem gradually approximates the solution to the original optimization problem (11). Furthermore, the optimal solution to each subproblem is also feasible to problem (11), since the feasible set of each subproblem is stricter than that of problem (11). As such, the proposed algorithm can obtain a suboptimal solution to the original optimization problem (11). The detailed algorithm is shown in Algorithm 1.

4 Numerical Results

In this section, we present the numerical results to demonstrate the performance of our proposed algorithm. For ease of presentation, the proposed algorithm, i.e., joint optimization of the UAV's trajectory and transmit power, is denoted as the JTPO scheme. For comparison, we consider a benchmark, i.e., transmit power optimization with fixed trajectory (denoted as the POFT scheme), where the transmit power is optimized by solving problem (25), and the line segment trajectory in [25] is adopted. The simulation parameters are set as: $P_{\max} = 20$ dBm, $\bar{P} = \frac{1}{2} P_{\max}$, $H = 100$ m, $\delta_t = 1$ s, $V_{\max} = 10$ m/s, $\xi_0 = 60$ dB, $\varepsilon = 10^{-5}$, $\epsilon = 10^{-2}$, $\tau = 10^{-6}$, $\mathbf{w}_b = [0, 0, 0]^T$ m, $\mathbf{w}_e = [400, 0, 0]^T$ m, $\mathbf{q}_I = [200, 100, H]^T$ m and $\mathbf{q}_F = [200, -100, H]^T$ m.

Fig. 2 plots the UAV trajectories obtained by the JTPO and the POFT schemes versus different flight duration T with blocklength $L = 400$. In this figure, when $T = 60$ s, we observe that the UAV first flies to a certain location around Bob at the maximum speed, then hovers at this location as long as possible, and finally flies to the final location at the maximum speed. We note that the hovering location is directly

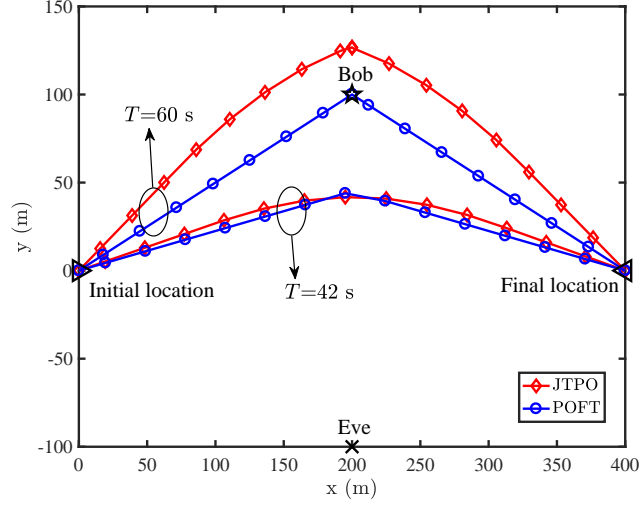


Figure 2 UAV trajectories sampled every 3 s for both schemes with $L = 400$.

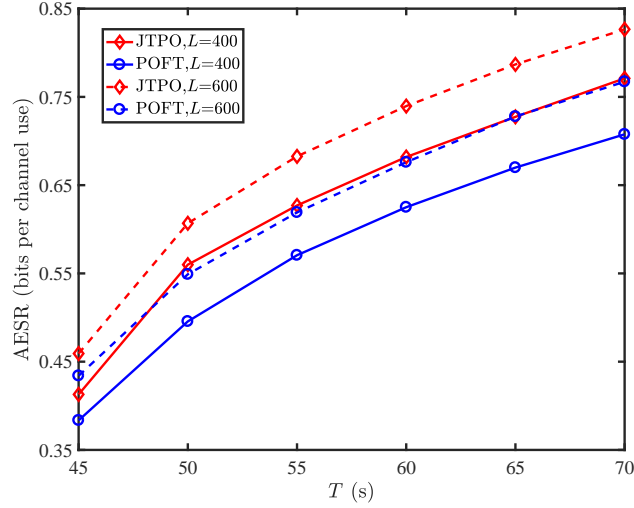


Figure 3 Average effective secrecy rate versus T .

above Bob while the eavesdropper is directly below Bob. As such, the hovering location is a tradoff between the communication performance and the secure performance. Compared with the line segment trajectory obtained by the POFT scheme, the trajectory obtained by our proposed scheme always flies away from Eve to degrade Eve's eavesdropping. When $T = 42$ s, the UAV is not allowed to fly to Bob due to the limited flight duration. Therefore, for both schemes, the UAV flies at the maximum speed from the initial location to the final location via different paths.

In Fig. 3, we plot the curves of AESR of both schemes versus different flight duration T . As expected, the JTPO scheme outperforms the POFT scheme thanks to the trajectory optimization. We can also observe that AESRs of both schemes increase as T increases because a larger T allows the UAV to hover at the hovering location for a longer time. In addition, AESRs obtained by both schemes increase as L increases, which is consistent with the results of (5).

Fig. 4 shows the transmit power of UAV over N time slots obtained by both schemes with $T = 60$ s and $L = 400$. We observe that Fig. 4 is symmetrical. Thus, we only analyze the first 30 time slots. In the first several time slots, we observe that the transmit power obtained by both schemes is equal to zero. This is because the rate from the UAV to Eve is higher than the rate from the UAV to Bob, which makes a positive secrecy rate cannot be guaranteed. Then, the UAV's transmit power increases as the UAV

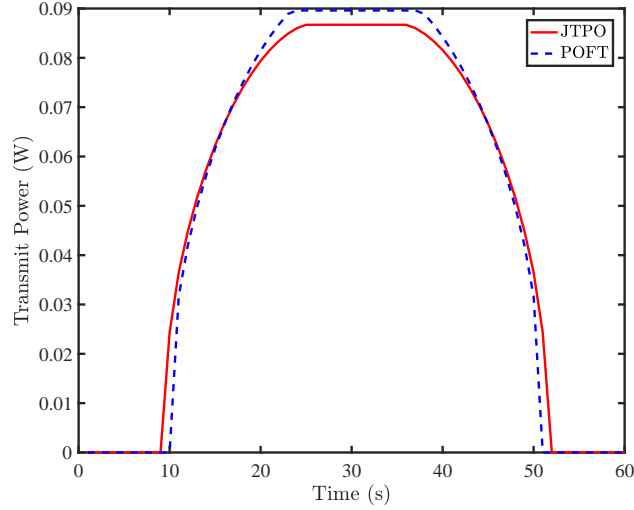


Figure 4 Transmit power for both schemes with $T = 60$ s and $L = 400$.

gets closer to Bob, and finally remains constant when the UAV reaches the hovering location. We also observe that both the proposed JTPO and the benchmark POFT schemes increase the transmit power of UAV when the UAV gets closer to Bob and reduce the transmit power of UAV when the UAV gets farther away from Bob.

5 Conclusions

In this paper, we investigated the UAV-enabled secure communication with finite blocklength. Under the condition of fixed blocklength, decoding error probabilities at Bob, and information leakage at Eve, we aimed to maximize AESR by jointly designing UAV's trajectory and transmit power. However, the resultant optimization problem was non-convex and difficult to solve directly. As such, we first decomposed the formulated optimization problem into the trajectory optimization and the transmit power optimization subproblems. Then we reformulated the two subproblems into convex optimization problems based on the first-order approximation technique. Finally, we developed an alternating iteration algorithm based on the SCA technique to solve the two subproblems iteratively. Numerical results showed that the proposed joint optimization scheme can achieve significantly better secure performance relative to a benchmark scheme.

References

- 1 Y. Zeng, R. Zhang, T. J. Lim. Wireless communications with unmanned aerial vehicles: opportunities and challenges. *IEEE Commun. Mag.*, 2016, 54: 36–42
- 2 M. Mozaffari, W. Saad, M. Bennis, et al. A tutorial on UAVs for wireless networks: applications, challenges, and open problems. *IEEE Commun. Surveys Tut.*, 2019, 21: 2334–2360
- 3 L. Gupta, R. Jain, G. Vaszkun. Survey of important issues in UAV communication networks. *IEEE Commun. Surveys Tut.*, 2016, 18: 1123–1152
- 4 S. Hayat, E. Yanmaz, R. Muzaffar. Survey on unmanned aerial vehicle networks for civil applications: a communications viewpoint. *IEEE Commun. Surveys Tut.*, 2016, 18: 2624–2661
- 5 Qualcomm and AT&T to trial drones on cellular network to accelerate wide-scale deployment. [Online] Available: <https://www.qualcomm.com/news/releases/2016/09/06/qualcomm-and-att-trial-drones-cellular-network-accelerate-wide-scale>
- 6 Paving the path to 5G: Optimizing commercial LTE networks for drone communication. [Online] Available: <https://www.qualcomm.com/news/onq/2016/09/06/paving-path-5g-optimizing-commercial-lte-networks-drone-communication>
- 7 Y. Zeng, R. Zhang, T. J. Lim. Joint trajectory and communication design for UAV-enabled multiple access. In: *Proceedings of IEEE Global Commun. Conf.*, Singapore, Singapore, 2017. 1–6
- 8 Q. Wu, Y. Zeng, R. Zhang. Joint trajectory and communication design for multi-UAV enabled wireless networks. *IEEE Trans. Wireless Commun.*, 2018, 17: 2109–2121

- 9 Y. Zeng, R. Zhang, T. J. Lim. Throughput maximization for UAV-enabled mobile relaying systems. *IEEE Trans. Commun.*, 2016, 64: 4983–4996
- 10 C. Zhan, Y. Zeng, R. Zhang. Energy-efficient data collection in UAV enabled wireless sensor network. *IEEE Wireless Commun. Lett.*, 2018, 7: 328–331
- 11 J. Zou, M. Wang, J. Zhang, et al. Discovery signal design and its application to peer-to-peer communications in OFDMA cellular networks. *IEEE Trans. Wireless Commun.*, 2013, 12: 3995–4009
- 12 Y. Zeng, R. Zhang. Energy-efficient UAV communication with trajectory optimization. *IEEE Trans. Wireless Commun.*, 2017, 16: 3747–3760
- 13 F. Shu, Y. Qin, T. Liu, et al. Low-complexity and high-resolution DOA estimation for hybrid analog and digital massive MIMO receive array. *IEEE Trans. Commun.*, 2019, 66: 2487–2501
- 14 F. Shu, L. Xu, J. Wang, et al. Artificial-noise-aided secure multicast precoding for directional modulation systems. *IEEE Trans. Veh. Technol.*, 2018, 67: 6658–6662
- 15 X. Zhou, J. Li, F. Shu, et al. Secure SWIPT for directional modulation-aided AF relaying networks. *IEEE J. Sel. Areas Commun.*, 2019, 37: 253–268
- 16 X. Zhou, S. Yan, Q. Wu, et al. Robust beamforming design for secure DM-based relay networks with self-sustained jammers. *IEEE Access*, 2019, 7: 969–983
- 17 F. Shu, X. Wu, J. Li, et al. Robust synthesis scheme for secure multi-beam directional modulation in broadcasting systems. *IEEE Access*, 2016, 4: 6614–6623
- 18 F. Shu, X. Wu, J. Hu, et al. Secure and precise wireless transmission for random-subcarrier-selection-based directional modulation transmit antenna array. *IEEE J. Sel. Areas Commun.*, 2018, 36: 890–904
- 19 J. Hu, S. Yan, F. Shu, et al. Artificial-noise-aided secure transmission with directional modulation based on random frequency diverse arrays. *IEEE ACCESS*, 2017, 5: 1658–1667
- 20 J. Hu, F. Shu and J. Li. Robust synthesis method for secure directional modulation with imperfect direction angle. *IEEE Commun. Lett.*, 2016, 20: 1084–1087
- 21 G. Zhang, Q. Wu, M. Cui, et al. Securing UAV communications via trajectory optimization. In: *Proceedings of IEEE Global Commun. Conf.*, Singapore, Singapore, 2017. 1–6
- 22 X. Zhou, Q. Wu, S. Yan, et al. UAV-enabled secure communications: Joint trajectory and transmit power optimization. *IEEE Trans. Veh. Technol.*, 2019, 68: 4069–4073
- 23 J. Hu, S. Yan, X. Zhou, et al. Covert wireless communications with channel inversion power control in rayleigh fading. *IEEE Trans. Veh. Technol.*, [Online] Available: <https://ieeexplore.ieee.org/document/8882293>
- 24 J. Hu, Y. Wu, R. Chen, et al. Optimal detection of UAV's transmission with beam sweeping in covert wireless networks. *IEEE Trans. Veh. Technol.*, [Online] Available: <https://ieeexplore.ieee.org/document/8887217>
- 25 X. Zhou, S. Yan, J. Hu, et al. Joint optimization of a UAV's trajectory and transmit power for covert communications. *IEEE Trans. Signal Process.*, 2019, 67: 4276–4290
- 26 J. Sachs, G. Wikstrom, T. Dudda, et al. 5G radio network design for ultra-reliable low-latency communication. *IEEE Network*, 2018, 32: 24–31
- 27 R. Chen, C. Li, S. Yan, et al. Physical layer security for ultra-reliable and low-Latency communications. *IEEE Wireless Commun.*, 2019, 26: 6–11
- 28 C. She, C. Yang, T. Q. S. Quek. Radio resource management for ultra-reliable and low-latency communications. *IEEE Commun. Mag.*, 2017, 55: 72–78
- 29 G. Durisi, T. Koch, P. Popovski. Toward massive, ultrareliable, and low-latency wireless communication with short packets. In: *Proceedings of IEEE*, 2016. 1711–1726
- 30 W. Yang, R. F. Schaefer, H. V. Poor. Finite-blocklength bounds for wiretap channels. In: *Proceedings of IEEE Int. Symp. Inf. Theory*, Barcelona, Spain, 2016. 3087–3091
- 31 H. Wang, Q. Yang, Z. Ding, et al. Secure short-packet communications for mission-critical IoT applications. *IEEE Trans. Wireless Commun.*, 2019, 18: 2565–2578
- 32 M. Grant and S. Boyd. CVX: Matlab software for disciplined convex programming. [Online] Available: <http://cvxr.com/cvx>, 2014